Correlation of Bubble-cap Fractionating-column Plate Efficiencies

EARL D. OLIVER and C. C. WATSON

University of Wisconsin, Madison, Wisconsin

A method of estimating the true conditions of operation of a bubble-cap tray is presented. Intermediate between the Murphree and the Lewis methods, which represent the extremes of actual operation, this method involves the use of a correlation to determine the degree of liquid mixing on the tray and the use of new relations between the Murphree vapor efficiency, the Lewis case I efficiency, and the true local efficiency. For the last, partial liquid mixing is taken into account.

Data were obtained on an 18-in. O.D. three-tray bubble-cap tower containing ten 3-in. bubble caps a tray. Partial liquid mixing was correlated for changes in vapor and liquid rates, pressure, temperature, and weir height for the system ethylene dichloride–toluene.

Efficiency data on acetone-water, ethanol-water, and ethylene dichloride–toluene showed the following effects: (1) low concentration of low boiler usually, but not always, resulted in low true local efficiencies, always with high Murphree efficiencies; (2) vapor velocity effects are more intimately connected with slot velocity than superficial velocity (and hence entrainment); (3) raising the pressure gives higher efficiencies; (4) an increase in liquid depth increases the true local efficiency but may have no effect on the Murphree efficiency.

THEORETICAL DEVELOPMENT

Murphree (*11*) assumed that the liquid on bubble-cap trays was completely mixed. Lewis (*10*) assumed that it was completely unmixed in the direction of flow. Actually, significant but incomplete liquid mixing was found in this study. The data were correlated by analogy to the well-known relation that the degree of mixing is a unique function of the power input per unit volume for a given geometrical shape and a given system. This led to a dimensionless mixing parameter,

$$F = f_1\left(\frac{u_G^2 w_G v_L}{2q_L^2 \mu_L}\right) \qquad (1)$$

In this parameter, $U_G^2 w_G/2q_L$ is considered the power input per unit volume of liquid per unit time, v_L/q_L is the residence time of the liquid, and μ_L is the resistance to mixing.

The Murphree vapor efficiency is, for Murphree's model, the ratio of actual to theoretical enrichment. Thus

$$E_{MV} = \frac{y_n - y_{n+1}}{y_n^* - y_{n+1}} \qquad (2)$$

Lewis (*10*) for his case I assumed (1) perfect vertical liquid mixing, (2) no horizontal liquid mixing (that is, in the direction of net cross flow), and (3) perfect mixing of entering vapor. On this model a material balance may be written for a differential slab between two vertical planes perpendicular to the direction of liquid flow, through which a differential amount of vapor dG rises. For constant molal overflow,

$$L\,dx = (y_n' - y_{n+1})\,dG = E_{OG}(y^* - y_{n+1})\,dG \qquad (3)$$

If E_{OG} is constant for the entire plate,

$$E_{OG} = \frac{L}{G}\int_{x_n}^{x_{n-1}} \frac{dx}{y^* - y_{n+1}} \qquad (4)$$

If the equilibrium line is straight for the concentration range involved,

$$E_{OG} = \frac{L}{mG}\ln\frac{y_{n-1}^* - y_{n+1}}{y_n^* - y_{n+1}} \qquad (5)$$

Combining with a material balance leads to

$$E_{OG} = \frac{y_n - y_{n+1}}{(y^* - y_{n+1})_{lm}} \qquad (6)$$

The denominator, which is the theoretical enrichment, is the logarithmic mean of the possible enrichment for the inlet and outlet liquid concentrations.

Lewis derived a relationship between his case I efficiency and the Murphree efficiency for a straight equilibrium line, as follows:

$$E_{OG} = \frac{\ln(1 + \lambda E_{MV})}{\lambda} \qquad (7)$$

In this work, for ethanol-water the integration of Equation (4) was performed by expressing the equilibrium data with Clark (*4*) equations and substituting for y^* in terms of x. Clark expressed binary equilibrium data by the equations

$$Y = AX + B \qquad (8a)$$

$$Y' = A'X' + B' \qquad (8b)$$

where

$$Y = y^*/(1 - y^*) = 1/Y'$$

$$X = x/(1 - x) = 1/X'$$

Equation (8*a*) is applicable above the conjugate, $X = \sqrt{A'B/AB'}$; Equation (8*b*) is applicable below. Both equations give an identical form to the integral, but the constants differ. Above the conjugate

$$E_{OG} = \frac{L}{G}\frac{1}{A_c}\left[A_a(x_{n-1} - x_n) + \frac{A}{A_c}\ln\frac{A_c x_{n-1} + A_d}{A_c x_n + A_d}\right] \qquad (9a)$$

where

$$A_a = A - B - 1$$

$$A_c = A - B - (A - B - 1)y_{n+1}$$

$$A_d = B - (B + 1)y_{n+1}$$

Below the conjugate

$$E_{OG} = \frac{L}{G}\frac{1}{A_c'}\left[A_a'(x_{n-1} - x_n) + \frac{A'}{A_c'}\ln\frac{A_c' x_{n-1} + A_d'}{A_c' x_n + A_d'}\right] \qquad (9b)$$

where

$$A_a' = 1 - A' + B'$$

$$A_c' = 1 - (1 - A' + B')y_{n+1}$$

$$A_d' = -A'y_{n+1}$$

For ethylene dichloride and toluene, y^* was related to x by an assumed constant relative volatility. Substitution and integration yield

Earl D. Oliver is with Shell Development Company, Emeryville, California.

Original data are contained in the Ph.D. thesis of Earl D. Oliver, which is obtainable on loan from the Memorial Library, University of Wisconsin, 728 State Street, Madison, Wisconsin.

$$E_{OG} = \frac{L}{G}\left[\frac{\alpha}{(C_1)^2}\ln\frac{C_1x_{n-1} - y_{n+1}}{C_1x_n - y_{n+1}} + \frac{(\alpha - 1)(x_{n-1} - x_n)}{C_1}\right] \quad (10)$$

where $C_1 = \alpha - (\alpha - 1)_{n+1}$.

For the system acetone-water, molal overflow was far from constant. An analysis similar to that resulting in Equation (3), but with all terms in the energy balance considered, yields for the top plate

$$\int_0^G \frac{E_{OG}\,dG}{L} = -\int_{x_0}^{x_1} \frac{dx}{y^* - y_2 - \frac{(H' - H_2)(y' - x)}{E_{OG}(H' - h)}} \quad (11)$$

The last term is considered a small correction term, and an average value is taken. Other approximations make possible the solution

$$E_{OG} = \frac{2}{G_2\left(\frac{1}{L_0} + \frac{1}{L_1}\right)} \cdot \int_{x_1}^{x_0} \frac{dx}{y^* - \left[y_2 + \frac{(H_1 - H_2)(y_1 - x_{1_{avg}})}{E_{OG}(H_1 - h_{1_{avg}})}\right]} \quad (12)$$

which is evaluated as in Equation (9).

On an actual plate a liquid concentration traverse would make possible a plot of y^* vs. distance across the plate, from which the theoretical enrichment could be derived. The ratio of the actual enrichment to the theoretical is the true local efficiency.

If only the total fractional mixing F is known, the assumption that the rate of mixing is uniform across the plate makes possible a solution analogous to Equation (4):

$$E_{OGT} = \frac{L}{G(1 - F)}\int_{x_n}^{x_0} \frac{dx}{y^* - y_{n+1}} \quad (13)$$

The previous integrations may be applied, or if the equilibrium line is straight, Equation (6) still holds, provided x_0 is used in place of x_{n-1} for finding the inlet equilibrium value. Alternatively, the true local efficiency may be derived from the Murphree efficiency as follows:

$$E_{OGT} = \frac{\ln\left[1 + \lambda(1 - F)E_{MV}\right]}{\lambda(1 - F)} \quad (14)$$

This equation reduces to the Lewis relation for $F = 0$, and, by L'Hôpital's rule, to $E_{OGT} = E_{MV}$ for $F = 1$.

The two-film theory of packed columns was extended to bubble-plate fractionating columns by Gerster et al. (*5*). Important equations may be combined in the following form:

$$N_{OG} = -\ln(1 - E_{OGT}) = \int_{y'_{n+1}}^{y'_n} \frac{dy'}{y^* - y'} = \frac{zK_{OG}a}{G} \quad (15)$$

Where liquid mixing occurs, the true local efficiency should be used as the measure of the actual number of transfer units. The composition y' represents the instantaneous bulk value for a single bubble, and y^* is the corresponding value in equilibrium with the adjacent liquid. Analogous relations may be written for the individual gas and liquid film resistances.

Certain limitations of Equation (15) should be carefully noted. In the first place the validity of the relation between N_{OG} and E_{OGT} depends on vertical constancy of liquid composition (and hence y^*). Direct determinations of point liquid compositions would present extreme experimental difficulties.

Second, the constancy of the transfer coefficient is doubtful, as, for example, the equations

$$\frac{1}{K_{OG}} = \frac{1}{k_G} + \frac{m}{k_L} \quad (16)$$

$$\frac{1}{N_{OG}} = \frac{1}{N_G} + \frac{mG}{L}\cdot\frac{1}{N_L} \quad (17)$$

The slope m is constant if the liquid composition is vertically constant. But the film transfer coefficients would be expected to depend on film properties. With interface equilibrium assumed in the two-film theory, the film concentration is necessarily variable.

Third, terms affecting interfacial area are not necessarily constant in bubble-plate columns.

Thus the two-film theory should not be thought of as basically sound. The simple flow pattern assumed in the derivation does not exist; nevertheless, the use of the two-film theory is a promising method of correlating efficiency data.

If efficiency data are to be generalized by the two-film theory, means must be available for predicting the interfacial area terms and transfer coefficient of Equation (15). No such means is available for the interfacial area terms, but the data of van Krevelen and Hoftijzer (*19*) suggest relative constancy at a given vapor rate on a given tray. Their data also indicate that the friction factor of a rising bubble is constant at high rates.

Variations of coefficients may be estimated by the Chilton-Colburn (*3*) modification of the Reynolds analogy. Thus

$$\frac{k_G}{G}\left(\frac{\mu_G}{\rho_G D_G}\right)^{2/3} = j_M = \frac{f}{2} \quad (18)$$

Generally the relation holds for skin friction, but not form drag. However, a bubble does not have a fixed shape, and its dimensions oscillate rapidly. Presumably both friction and mass transfer are increased by the greater turbulence.

If the mass transfer factor is assumed constant, one may obtain

$$k_G = C_2\frac{\rho_G u_G}{M_G}\left(\frac{\mu_G}{\rho_G D_G}\right)^{-2/3} \quad (19)$$

This assumption gives a much more reasonable function of the viscosity than does the assumption that mass transfer data for solid particles apply. Such data make the mass transfer factor proportional to the $-\frac{1}{2}$ power of Reynolds number, which would nearly cancel the effect of viscosity shown in Equation (19).

For constant-rate data on a given system, with the perfect gas law assumed and diffusivity taken proportional to the temperature to the $\frac{3}{2}$ power divided by the pressure, Equation (19) reduces to

$$k_G = C_3 p_t^{1/3}\left(\frac{\mu_G}{\rho_G}\right)^{-2/3} \quad (20)$$

For the liquid film, in the same way,

$$k_L = C_4\frac{\rho_L u_L}{M_L}\left(\frac{\mu_L}{\rho_L D_L}\right)^{-2/3} \quad (21)$$

For constant-rate data

$$k_L = \frac{C_5}{V_L}\left(\frac{\mu_L}{\rho_L D_L}\right)^{-2/3} \quad (22)$$

Frequently for a liquid $D\mu/T$ is constant. If so,

$$k_L = \frac{C_6}{V_L}\left(\frac{\mu_L^2}{\rho_L T}\right)^{-2/3} \quad (23)$$

It is not clear whether the velocities in these equations are rising bubble velocities, relative velocities of vapor to liquid, or some other velocities. Frequent reports of relatively constant efficiency over a wide range of velocity suggest that whatever velocities are effective are often constant in this range.

Also, fairly successful correlations which neglect design factors suggest that efficiencies may be generalized by consideration of the effects of Equations (20) and (22) only.

EXPERIMENTAL WORK

Apparatus

A fractionating column of 18-in. O.D. and 300 lb./sq. in. gauge rating was used. It contained three trays at 2-ft. spacing, with ten 3-in. bubble caps a tray on 4½-in. equilateral triangular centers. The equipment was originally the same as was used by Shilling, Beyer, and Watson (*18*), and further constructional details may be obtained from their paper. Changes made in their equipment will be noted.

The sampling arrangements intended to measure point efficiencies directly proved entirely inadequate at rates higher than those used in the prior work, probably because of the unpredictable blowing of the liquid away from the sampler. The vapor chimney was therefore removed and the vapor sampler made movable, to make vapor-composition traverses possible. Late in the work the liquid sampler (Shilling x_c)

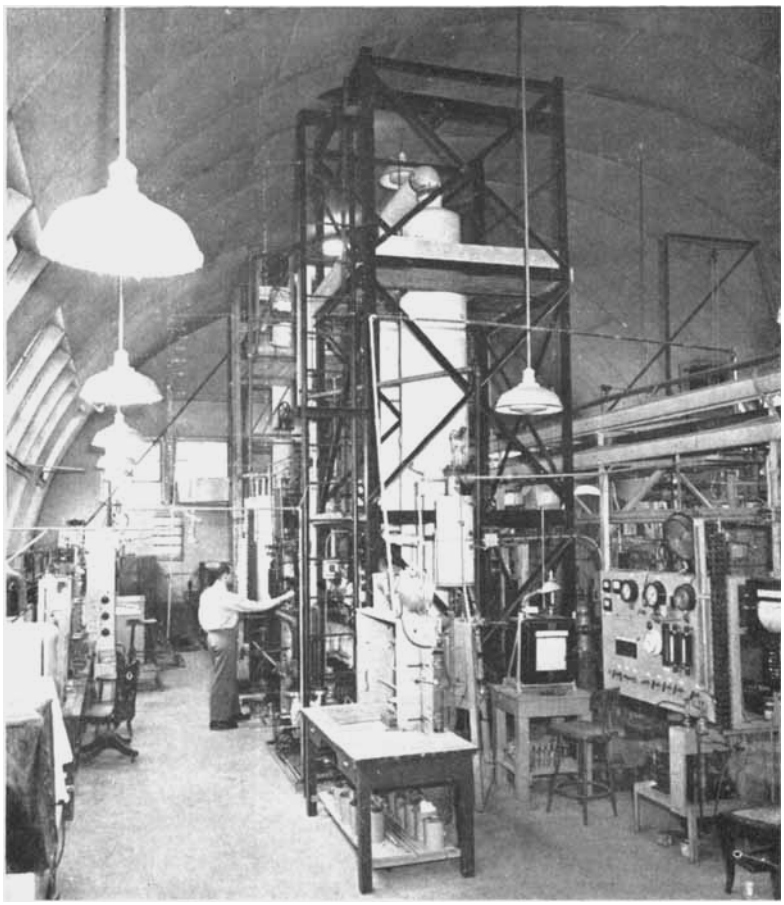

Fig. 1. Over-all view of apparatus.

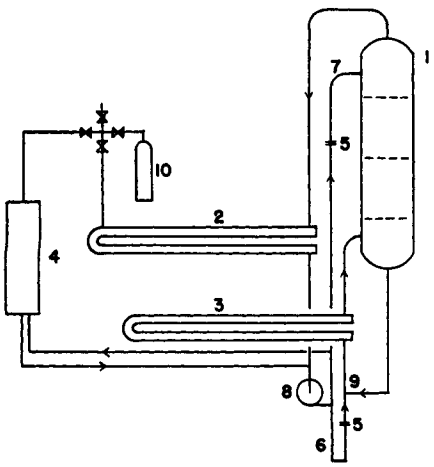

Fig. 2. Flow diagram.

1. Fractionating column
2. Condenser
3. Reboiler
4. Surge tank
5. Orifice meters
6. Product line
7. Reflux line
8. Reflux pimp
9. Jet pump connection
10. Nitrogen supply

was moved so as to draw liquid from just downstream of the inlet weir. The composition of this sample was the basis of the fractional mixing.

For some of the later runs a hinged gate was installed above the outlet weir on the middle tray only. In the closed position it raised the weir height to 2 in. Weir length was reduced to 6 in. to allow room for the supports.

For studying the effect of vapor velocity, the relation between slot velocity and superficial velocity was changed markedly by blocking flow through 40% of the slots. All the liquid was still forced to flow past the active slots. The top two trays were modified identically. The three caps on the east side (weirs were on north and south sides) were plugged in the risers, and a sheet-metal dam was installed to prevent liquid from flowing past these caps. On the west side the two caps nearer the outlet weir had half their slots facing outward blanked. Dams were built to prevent liquid flow past the inactive slots. Sheet-metal inserts in the risers for these half-blanked caps cut the flow area in half. Asbestos rope was used to seal the dams.

Changes and additions to auxiliary equipment increased the capacity for condensation, reboiler circulation, and pumping.

A general view of the equipment is shown in Figure 1.

Procedures

Figure 2 is a flow diagram of the equipment as operated. With this arrangement steady conditions were possible at either total or partial reflux without a large inventory of charge stock.

Reflux temperature was controlled by a steam jacket on the reflux, the steam being controlled by a globe valve. To make the top plate comparable to the middle plate, it was attempted to return reflux at just below the bubble-point temperature. When this condition could not be achieved, and it appeared that top-plate efficiencies were adversely affected, they were not plotted with the others. Pressure was controlled by opening the condenser vents to the atmosphere for operation or by closing the vents and introducing nitrogen for other pressures. Flows were controlled by globe valves. Rates were determined from the pressure drops across orifices, as measured by mercury manometers. Valves in the manometer leads were opened early in the run to ensure that liquid in the leads was the same as reflux.

Samples were drawn at rates which were small fractions of the total rates, so as not to disturb the steady-state conditions. Unless something interfered, all runs were checked by separate sets of samples and readings of instruments at least ½ hr. apart. The first set of samples was generally not taken until conditions had been reasonably steady for at least 1 hr. It was necessary to adjust flows and heat input by trial to get the desired conditions.

Ethanol–water samples were analyzed by density, which was measured by a Westphal balance of chainomatic type at room temperature. Errors due to change in composition during this operation and during sampling were shown experimentally to be insignificant. Data from Perry (*14*) were used to find the composition.

Acetone–water samples were also analyzed by density, with the same balance, but at 0°C. to minimize errors due to the higher volatility. Data of Schwers (*17*) were used to find the concentration corresponding to a given density.

Ethylene dichloride–toluene samples were analyzed by means of an Abbé refractometer. Data of Jones et al. (*8*), together with direct experimental data, were used to determine the composition from the refractive index.

CALCULATIONS

Ethanol-water

Flow rates for all systems were calculated from standard orifice equations, with upstream velocity head considered, a discharge coefficient of 0.61, which was determined by calibration, being used. Liquid in the manometer leads was assumed to be reflux at room temperature. Flowing liquid temperature was measured, and the density at that temperature used. Reflux and "product" rates were obtained in this way; other rates were calculated by material and energy balances.

Slot velocities were based on total slot area, as the slots were generally fully open, and major interest was in conditions where they were. "Allowable" velocities were calculated by the method outlined in Perry (*14*).

It has often been pointed out that the equilibrium data used in calculating plate

efficiencies are fully as important as the experimental data themselves. Consequently much effort was directed toward examining and comparing data from different sources. Rao (*15*) has obtained excellent averaging of all available equilibrium data on the ethanol-water system, using Clark equations developed by the method of least squares. In addition, he tested the equations by calculating temperatures and using the Gibbs-Duhem relation. His equations are

$$Y = 0.8853X + 0.9701 \text{ (above conjugate)}$$

$$Y' = 0.07755X' + 0.5709 \text{ (below conjugate)}$$

The conjugate point is at $x = 0.2796$.

Another test made by the authors was based on the thermodynamic equation

$$\int_0^1 \ln \frac{\gamma_1}{\gamma_2}\, dx = 0$$

This expression has the advantage of not requiring evaluation of any slopes, which makes results of the usual Gibbs-Duhem form uncertain. The value of the integral was 0.0045 instead of zero. Thus, if the error is constant for the whole composition range, γ_1/γ_2 is high by 0.45%. This is the error in relative volatility, with the error in y^* being smaller yet. Apparently Rao's equations give the best representation of ethanol-water equilibrium now available.

Another advantage of this manner of expressing data is that the mathematical form allows direct evaluation of the integral of Equation (4). In collaboration with Rao, the authors computed values of this integral for various arbitrary values of the parameters and plotted them as illustrated in Figure 3. The value of the integral between any two points for a given y is quickly found as the difference between the corresponding ordinates on the plot. A more detailed large-scale plot was used in the actual calculations of Lewis case I efficiencies by Equation (4).

A Ponchon-Savarit diagram was constructed for the ethanol-water system by transposing the data of White (*20*) to a molar basis. Murphree vapor-plate efficiencies were calculated by use of the Ponchon-Savarit diagram to find the vapor compositions from the liquid compositions, which were found to be more reliable than measured vapor concentrations, and by use of the Clark equations to find the equilibrium values.

Acetone-water

Data of the International Critical Tables (*7*) were used to construct a Ponchon-Savarit diagram, employed to find enthalpy values as well as vapor compositions.

Clark equations were developed by averaging the data of Brunjes and Bogart (*1*); Othmer, Friedland, and Scheibel (*13*); Othmer and Benenati (*12*); and York and Holmes (*21*). The results were

$$Y = 1.151X + 4.485 \text{ (above conjugate)}$$

$$Y' = 0.02553X' + 0.1532 \text{ (below conjugate)}$$

The conjugate is at $x = 0.4464$.

Testing with the Gibbs-Duhem equation indicated that these equations are slightly less consistent than the best experimental data. The value of

$$\int_0^1 \ln \frac{\gamma_1}{\gamma_2}\, dx$$

was 0.053. The error is unfortunately large, but the calculated curve falls within the experimental-data band at all concentrations. Because of the convenience of the expressions, they were used.

Figure 4 gives the integral of Equation (4) for the acetone-water system.

Other calculations were parallel to those for the ethanol-water system, except that Equation (12), or its equivalent for the middle tray, was used to find the Lewis case I efficiency. Equation (6) was used for the true local efficiency for actual liquid concentrations, which was spot-checked by Equation (13).

Ethylene Dichloride–Toluene

This system was assumed ideal whereever enthalpy data were required. Necessary data were obtained from Perry (*14*), Lange (*9*), and A.P.I. Project 44 (*2*).

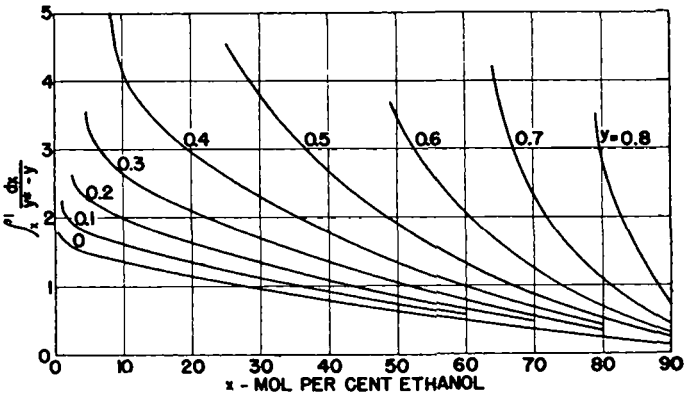

Fig. 3. $\int_x' dx/(y^* - y)$ for ethanol-water system.

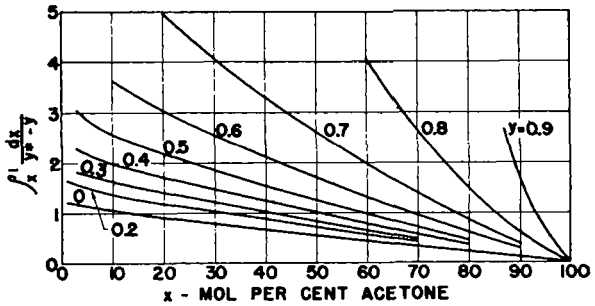

Fig. 4. $\int_x' dx/(y^* - y)$ for acetone-water system.

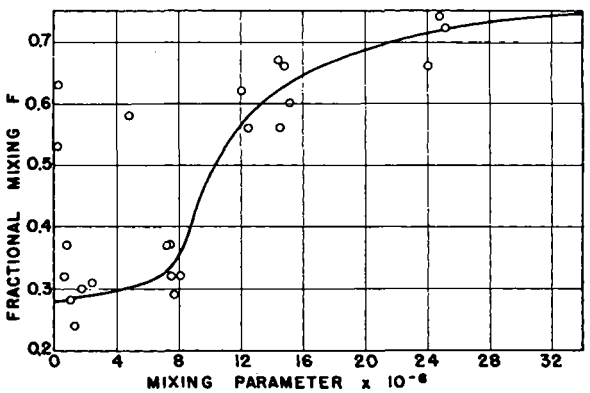

Fig. 5. Effect of the mixing parameter [Equation (1)] on fractional mixing for the ethylene dichloride-toluene runs.

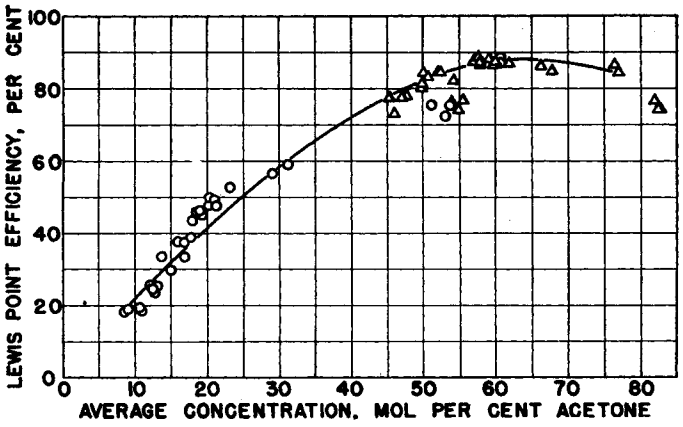

Fig. 6. Acetone–water runs, concentration study. Triangles are for top plate, circles for middle plate; reflux ratio $L_0/D = \frac{1}{2}$; atmospheric pressure; vapor rate about 24 lb.-moles/hr.; Lewis case I assumptions made; static seal $\frac{1}{2}$ in.

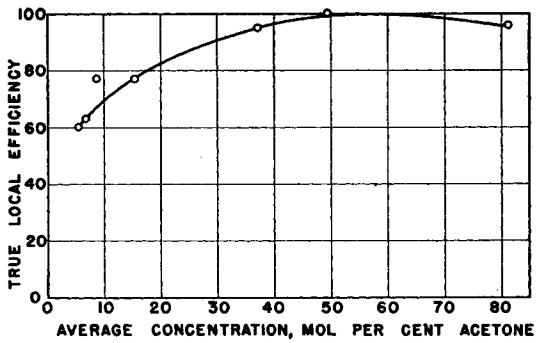

Fig. 7. Effect of concentration of acetone on true local efficiency.

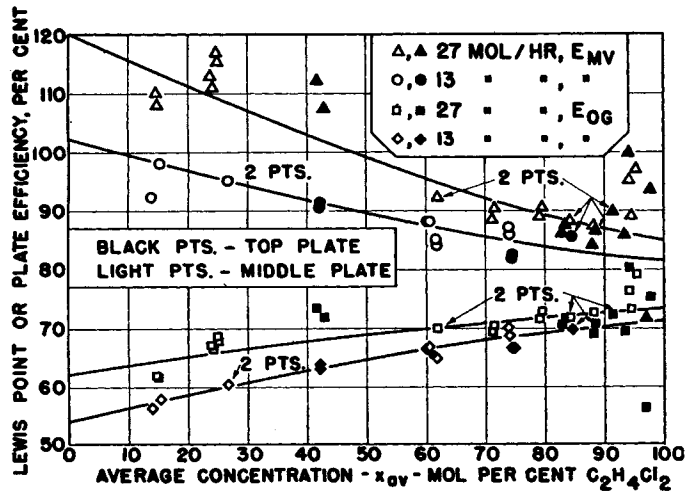

Fig. 8. Effect of concentration of ethylene dichloride on Lewis point efficiency and on plate efficiency.

Jones, Schoenborn, and Colburn (*8*) found that this system follows Raoult's law. Accordingly for atmospheric pressure, equilibrium data were calculated with ideal mixtures and ideal gas vapors assumed. For higher pressures corrections to vaporization equilibrium constants were combined as a correction to relative volatility by use of the generalized charts of Hougen and Watson (6). Relative volatilities were plotted and used to calculate point efficiencies by Equation (10).

Vapor compositions were found from liquid compositions by a McCabe-Thiele diagram.

When the composition just downstream of the inlet weir was available, the true local efficiency of the middle tray was calculated by Equation (13) and/or (14).

The vapor velocity for the mixing correlation was based on the plate free area, defined as the total area between the weirs minus the area of the caps.

The liquid holdup on the tray was assumed to be the plate free area times the height of the weir. The true holdup is probably roughly proportional to this term for a plate having a baffle by the outlet weir, as this one did.

RESULTS

Mixing of Liquid

Figure 5 shows that the mixing of the liquid was always between one quarter and three quarters complete on this tray; that is, the concentration change across the inlet weir was one quarter to three quarters the total between the two plates. (This maximum mixing held to a value of the mixing parameter of 140 million, which is well beyond the range plotted.) The fractional mixing F may theoretically vary from zero to one. Zero corresponds to a Lewis plate; one to a Murphree plate. Such data were obtained for the system ethylene dichloride–toluene only, for one particular tray. Conditions which were varied included vapor and liquid flow rates, pressure, temperature, and weir height.

The accuracy of the mixing correlation is questionable. The band of points is rather wide, but this is more likely the result of experimental errors than of ascribing the wrong effects to the different variables. Thus instantaneous concentrations at a point were found, under some conditions, to vary 5% or more within a matter of seconds. Eddying is known to occur near weirs, and there is no assurance that the sampler was in the same position in the eddy under different conditions. This correlation should not be applied indiscriminately to other trays until the effect of tray size and geometry is studied. The evidence is strong, however, that under no normal operating conditions does this plate resemble either a Murphree or a Lewis plate. It is in between the two.

Mixing of Vapor

Variations in the composition of the vapor entering a tray appear to have little effect. Although composition traverses under conditions of appreciable liquid entrainment gave erratic results, lower rate runs showed nearly uniform composition. Vapor composition may vary more for plate spacings less than the 2 ft. of this column. The Lewis case III plate, however, in which the vapor is assumed unmixed, generally shows little advantage over the case I plate, in which the vapor is assumed completely mixed.

Concentration

Acetone-water. A low concentration of acetone in water gives a low Lewis case I efficiency, as shown in Figure 6. The drop at low concentrations has been attributed to the increase in the liquid film resistance from the higher liquid viscosity and larger value of the slope of the equilibrium line. The larger slope is analogous to a lower solubility of acetone vapor. Equation (16) shows its effect.

The effect of concentration of acetone on true local efficiency, in which liquid mixing is taken into account, is less pronounced, as shown in Figure 7. Thus the large variation of Lewis case I efficiency is the result not only of the effect of the slope m on the liquid-film resistance, but also of the effect of slope m on the calculation of efficiencies from experimental measurements.

The data of Shilling, Beyer, and Watson (*18*) confirm this conclusion. Their plot of point efficiencies, i.e., those determined from liquid and vapor samples at the center of the tray, shows much less variation than does the plot of local efficiencies, i.e., those determined from exit liquid samples by means of the Lewis analysis.

The curve in Figure 7 was derived by assuming that the liquid was three quarters mixed, which was indicated by the mixing correlation based on ethylene dichloride and toluene data. A few points falling on the Lewis case I curve were recalculated to give the new curve. Both the ordinate and abscissa for a given run will be different from those in Figure 6. The abscissa is the average liquid composition on the tray, consistent with the assumptions used in deriving the efficiencies. The assumption that local efficiency is constant across the tray, which was necessary to perform the integration, is obviously not true, because composition may vary widely across the tray. This method of plotting is intended to cancel out as much of the error introduced as possible. It has the property of moving points out much farther from the ordinate axis at low concentrations than when exit liquid concentration is the abscissa.

Lewis case I efficiencies are easiest to correlate, because the spread of liquid composition is the greatest. Hence the average value of the equilibrium vapor composition is least dependent on experimental liquid compositions.

Ethylene Dichloride–toluene. The curves of Figure 8 show the trends anticipated from the two-film theory and the Lewis analysis. Thus a large slope of the equilibrium line (low concentration) corresponds to a large Murphree efficiency but a small Lewis case I efficiency. Equation (7) predicts the former effect; Equations (17) and (15) predict the latter.

A plot of true local efficiencies, as in Figure 9, however, is quite surprising. The 27 moles/hr. data show that this efficiency is definitely higher at low concentrations than at high. Equation (17) is unable to predict this. One must assume that the interfacial area terms of Equation (15) are responsible. In contrast to the 27 moles/hr. data, the 13 moles/hr. data show the expected trend.

To find whether the 27 moles/hr. trend might be explained by errors in the experimental mixing data used, the true local efficiencies at 0 and 100% ethylene dichloride were calculated from extrapolated Lewis case I efficiencies and the mixing correlation. These true local efficiencies were 0.91 and 0.81, respectively, confirming the previous conclusion. The extrapolation, however, was somewhat uncertain.

Vapor Velocity

Acetone-water. The slot velocity appears to be more important than superficial column velocity to plate performance, as shown in Figures 10 and 11. They include efficiencies in the concentration range of 60 to 75% acetone, where the effect of concentration was small. Also, the mixing correlation indicates that the liquid was about three quarters mixed in all these runs. Hence it is permissible to show the trends by plotting any convenient efficiency.

Figure 10 is derived from the traditional method of finding the capacity of a column, based on the idea that entrainment causes the loss in efficiency above the normal operating range. The plot shows very clearly that more is involved than entrainment, because otherwise a single line should be obtained for both sets of data. The comparability of the two sets of data is established by the check obtained at low rates.

Figure 11 is based on the idea that "coning," the pushing back of liquid from the slots, is more likely to be the limiting condition. Here the two sets of data form a single line, establishing $\rho_G V_S^2$ as a better criterion of the effect of vapor velocity on efficiency.

Ethanol-water. The preferability of the slot-velocity-head criterion is confirmed by Figure 12. The data fall near a single curve. They would not for a superficial velocity-head criterion. For a given slot velocity head, the superficial velocity head is 36% as much for partial slot operation as for total slot operation.

The efficiencies plotted were for the concentration range of 30 to 40% ethanol, where concentration has little effect. The

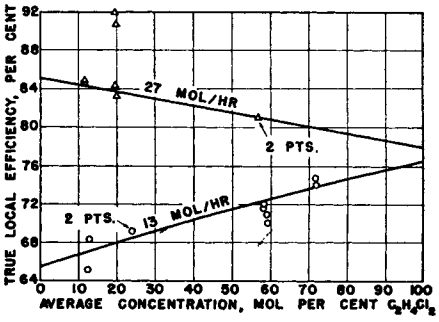

Fig. 9. Effect of concentration of ethylene dichloride on true local efficiency.

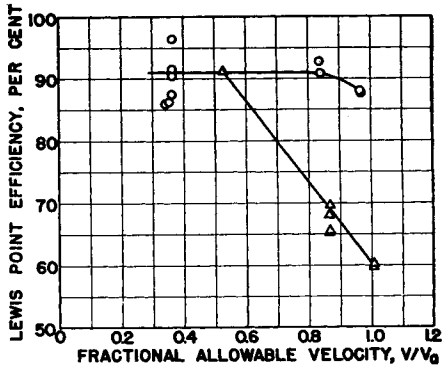

Fig. 10. Effect of slot velocity on Lewis point efficiency.

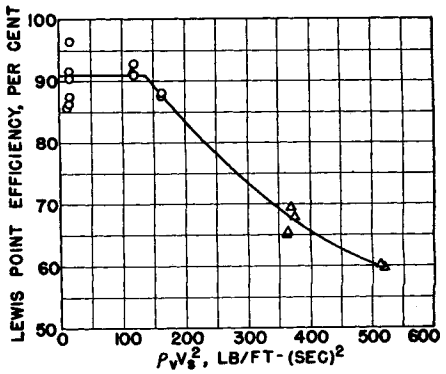

Fig. 11. Acetone–water runs, vapor velocity study. For circles, all slots were active; for triangles, 40% of slots were blocked; same data as Fig. 10.

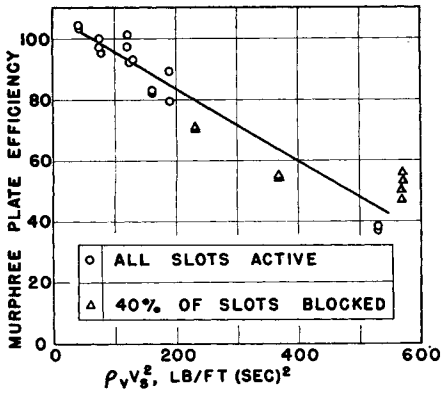

Fig. 12. Correlation of Murphree plate efficiency for ethanol-water with slot-velocity head.

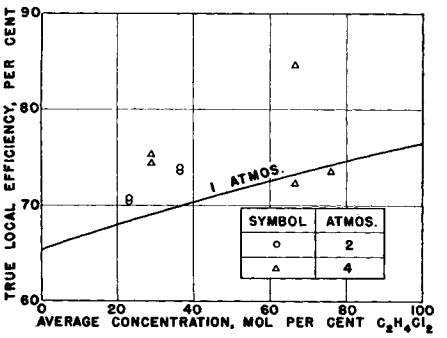

Fig. 13. Effect of pressure on true local efficiency for ethylene dichloride-toluene.

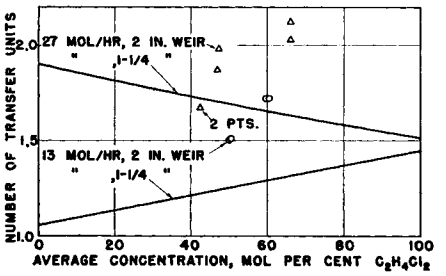

Fig. 14. Effect of liquid depth on true local efficiency for ethylene dichloride-toluene.

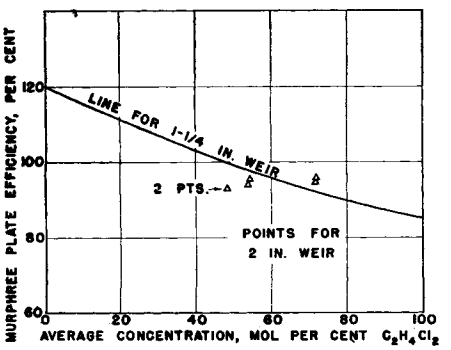

Fig. 15. Effect of liquid depth on Murphree plate efficiency for ethylene dichloride-toluene.

low reflux ratios used, which were necessary to get enough reboiler circulation, reduced the accuracy of these data.

At the highest slot velocity heads, total slot operation gave lower efficiencies. The greater entrainment was no doubt responsible.

Ethylene Dichloride-toluene. Efficiencies are higher at 27 moles/hr. (two thirds the "allowable") than at 13 moles/hr., as shown in Figures 8 and 9. This is in contrast to some other systems. Data taken in the study of pressure confirm that higher rates give higher efficiencies when the column is well below capacity.

Pressure

Increasing the pressure increases the true local efficiencies at constant rate and composition for the system ethylene dichloride-toluene, as shown in Figure 13 and Table 1.* This effect is attributed mainly to the lower kinematic viscosities of both the liquid and vapor phases. The slope, m, becomes lower at low concentrations, but higher at high concentrations as pressure rises. Figure 13 also gives the atmospheric pressure lines from Figure 9, with the points omitted to avoid confusion.

This study was hampered by the inability to get the desired vapor rates at the lower reboiler temperature differences and by the difficulties of operating at the ultimate heat transfer capacity. The experimental mixing data were erratic for the superatmospheric pressure runs, and so the correlation values of mixing were used in calculating the true local efficiencies.

Some anomalies appear in the data. These are mainly in the low separation regions of high concentration, where accuracy is poor. Also, the 2-atm. 27 moles/hr. data are not consistently above the 1-atm. data in this plot. Use of the experimental mixing values in place of the correlation on values, however, would make the 2-atm. data higher.

Because of the large effects of vapor rate and concentration, pressure effects should not be inferred unless the other conditions are constant.

Liquid Depth

Increasing the liquid depth increases the true local efficiency. The number of transfer units is shown in Figure 14 for two weir heights, namely, 1¼ and 2 in. The corresponding static seals are ½ and 1¼ in.

Gilliland (*16*) has suggested that the number of transfer units should be taken as proportional to the square root of the average slot submergence. This is not a bad approximation for these data.

The efficiency that really counts, however, was not increased at all for the 27 moles/hr. runs. The degree of mixing increased as well as the true local efficiency, and so the Murphree vapor efficiency received no net benefit. From an operational standpoint, the higher weir would be of no advantage. To illustrate this point, the 2-in. weir data are plotted in Figure 15 together with the 1¼-in. weir line from Figure 8.

QUANTITATIVE CORRELATIONS OF RESULTS

Equations from the section on theoretical development have been successfully used to predict variations of performance for constant vapor velocity data. Illustrations are given below for changes in composition and pressure.

A single efficiency point cannot be separated into individual film resistances and Equation (17) applied. However, if the modes of variation of resistances are known, the resistances at another point may be expressed in terms of those of the first, and the two equations may be solved simultaneously.

In total reflux runs the vapor entering a tray has the same composition as the liquid leaving the tray. These compositions are used to estimate properties in the following calculations.

For analysis of the 13 moles/hr. data of Figure 12, subscript 0 refers to conditions at 0% ethylene dichloride. Equation (17) becomes

$$0.943 = \frac{1}{N_{GO}} + 2.12\left(\frac{1}{N_{LO}}\right) \quad (24)$$

Subscript 1 identifies any other condition for the constant rate data. Equations (20) and (22) lead to the relation

$$\frac{1}{N_{OG_1}} = \frac{1}{N_{G_0}}\left(\frac{P_{t_0}}{P_{t_1}}\right)^{1/3}\left(\frac{\nu_{G_1}}{\nu_{G_0}}\right)^{2/3} + \frac{m_1 G_1}{L_1}\left(\frac{1}{N_{L_0}}\right)\left(\frac{V_{L_1}}{V_{L_0}}\right)\left(\frac{\nu_{L_1} D_{L_0}}{\nu_{L_0} D_{L_1}}\right)^{2/3} \quad (25)$$

Assuming liquid diffusivities constant and substituting numerical values at 100% ethylene dichloride yield

$$0.690 = \frac{1}{N_{G_0}}\left(\frac{3.20}{3.05}\right)^{2/3} + 0.435\left(\frac{1}{N_{L_0}}\right)\left(\frac{84.0}{118}\right)\left(\frac{0.35}{0.32}\right)^{2/3} \quad (26)$$

Solving Equations (24) and (26) simultaneously gives values for $1/N_{L_0}$ of 0.153 and for $1/N_{G_0}$ of 0.618.

If these values are used, Equation (25) will predict for 50% ethylene dichloride.

$$\frac{1}{N_{OG_1}} = 0.618\left(\frac{3.12}{3.05}\right)^{2/3} + 0.856(0.153)\left(\frac{101}{118}\right)\left(\frac{0.34}{0.32}\right)^{2/3}$$

$$= 0.743$$

*See footnote on page 18.

The corresponding value of E_{OGT} is 0.740, compared with the experimental value of 0.715.

This type of comparison is obviously dependent on the values used for the physical properties. Lack of knowledge about liquid diffusivities makes the liquid-phase resistance uncertain. This resistance is indicated, however, to vary from 35% of the total at 0% concentration down to 10% at 100% concentration.

For these data, liquid- and gas-phase kinematic viscosities varied in about the same ratio. A better check on the effect of kinematic viscosity will be to compare data at different pressures but at the same composition, provided the relative phase resistances are reasonably accurate. Because of the compressibility of the gas, its kinematic viscosity falls much more rapidly than that of the liquid. Variations of diffusivity can be predicted when only the temperature and pressure change.

The 27 moles/hr., 2-atm. curve is chosen to compare with the 13 moles/hr. atmospheric curve, because it is at about the same volumetric vapor rate. By Equations (20) and (23),

$$\frac{1}{N_{OG_1}} = \frac{1}{N_{G_0}}\left(\frac{P_{t_0}}{P_{t_1}}\right)^{1/3}\left(\frac{\nu_{G_1}}{\nu_{G_0}}\right)^{2/3} + \frac{m_1 G_1}{L_1}\left(\frac{1}{N_{L_0}}\right)\left(\frac{V_{L_1}}{V_{L_0}}\right)\left(\frac{\rho_{L_0} T_0}{\rho_{L_1} T_1}\right)^{2/3}\left(\frac{\mu_{L_1}}{\mu_{L_0}}\right)^{4/3} \quad (22)$$

When the atmospheric values already determined at 0% ethylene dichloride are used, the over-all resistance at 2 atm. would be predicted as

$$\frac{1}{N_{OG}} = 0.618\left(\frac{1}{2}\right)^{1/3}\left(\frac{1.62}{3.05}\right)^{2/3} + 1.905(0.153)\left(\frac{123}{118}\right)\cdot\left[\left(\frac{0.781}{0.746}\right)\left(\frac{384}{410}\right)\right]^{2/3}\left(\frac{0.20}{0.25}\right)^{4/3} = 0.544$$

$$E_{OGT} = 0.841$$

The mixing correlation indicates that F is 0.30. The predicted Murphree vapor efficiency by Equation (14) is 155%, which may be compared with the extrapolated experimental value of 152%.

This research indicates that at least three types of data should be taken in future work, if possible: first, plate efficiencies; second, mixing data; and third, interfacial areas.

ACKNOWLEDGMENT

Financial support of the Shell Fellowship Committee, the Chemical Engineering Department of the University of Wisconsin, and the Wisconsin Alumni Research Foundation is gratefully acknowledged.

M. N. Rao helped in the treatment of equilibrium data and collaborated in the evaluation of integral functions for the system ethanol–water.

NOTATION

a = surface area per unit volume, sq. ft./cu. ft.
A, A', B, B' = constants in Clark equations
A_a, A_b, A_c, A_d, B_d, B_b, B_c, B_d, c_1, etc. = constants as defined
D = diffusivity
E_{MV} = Murphree vapor plate efficiency
E_{OG} = local efficiency by Lewis case I analysis
E_{OGT} = true local efficiency
f = Fanning friction factor
f_1, etc. = function
F = fractional mixing, concentration change across inlet weir divided by total change across plate,

$$F = \frac{X_n - X_e}{X_n - X_{n+1}}$$

G = mass velocity of vapor, lb.-moles/(hr.)(sq. ft.)
h = enthalpy of liquid, B.t.u./mole
H = enthalpy of vapor, B.t.u./mole
j_M = mass transfer factor
k_G = mass transfer coefficient, moles/(hr.)(sq. ft.)$(y_i - y)$
k_L = mass transfer coefficient, moles/(hr.)(sq. ft.)$(x - x_i)$
k_{OG} = mass transfer coefficient, moles/(hr.)(sq. ft.)$(y^* - y)$
L = mass velocity of liquid, lb.-moles/(hr.)(sq. ft.)
m = dy^*/dx, slope of equilibrium line
M = molecular weight
N_G = number of gas-phase transfer units
N_L = number of liquid-phase transfer units
N_{OG} = number of over-all transfer units, based on gas phase
P_t = total pressure
P_1 = vapor pressure, low boiler
P_2 = vapor pressure, high boiler
q = volumetric flow rate, cu. ft./sec.
T = absolute temperature
u = local velocity
V = superficial column velocity, ft./sec.
V_a = allowable superficial column velocity, ft./sec.
V_S = slot velocity, ft./sec.
V_G = molal volume, gas
V_L = molal volume, liquid
v_L = volume of liquid holdup on tray, cu. ft.
w = mass flow rate, lb./sec.
x = mole fraction, liquid
x_e = mole fraction in liquid, just downstream of inlet weir
X = mole ratio, liquid
y = mole fraction, vapor, average
y' = mole fraction, vapor, at a point
y^* = mole fraction, vapor, in equilibrium with liquid at that point
Y = mole ratio, vapor
Z = distance, vertical direction, ft.
α = relative volatility
γ_1 = activity coefficient, low boiler
γ_2 = activity coefficient, high boiler
λ = mG/L
μ = viscosity (dynamic)
ρ_V = density, vapor
ρ_L = density, liquid
ν = viscosity, kinematic

Subscripts

0, 1, 2, 3 = reflux, top, middle, bottom tray, for flow quantities, thermodynamic functions, and concentrations
n = number of tray, down from top
L = liquid
G = gas
OG = over-all, based on gas film
V = vapor
i = interface between phases
avg = average
l.m. = logarithmic mean
e = entering plate
$'$ = (prime) point condition

LITERATURE CITED

1. Brunjes, A. S., and M. J. P. Bogart, *Ind. Eng. Chem.*, **35**, 255 (1943).
2. Bur. Standards, "Selected Values of Properties of Hydrocarbons," U. S. Govt. Printing Office, Washington (1947).
3. Chilton, T. H., and A. P. Colburn, *Ind. Eng. Chem.*, **26**, 1183 (1934).
4. Clark, A. M., *Trans. Faraday Soc.*, **41**, 718 (1945); **42**, 742 (1946).
5. Gerster, J. A., A. P. Colburn, W. E. Bonnet, and T. W. Carmody, *Chem. Eng. Progr.*, **45**, 716 (1949).
6. Hougen, O. A., and K. M. Watson, "Chemical Process Principles," John Wiley and Sons, New York (1947).
7. "International Critical Tables," McGraw-Hill Book Company, Inc., New York (1926).
8. Jones, C. A., E. M. Schoenborn, and A. P. Colburn, *Ind. Eng. Chem.*, **35**, 666 (1943).
9. Lange, N. A., "Handbook of Chemistry," 4 ed., Handbook Publishers, Inc., Sandusky, Ohio (1941).
10. Lewis, W. K., *Ind. Eng. Chem.*, **28**, 399 (1936).
11. Murphree, E. V., *Ind. Eng. Chem.*, **17**, 747 (1925).
12. Othmer, D. F., and R. F. Benenati, *Ind. Eng. Chem.*, **37**, 299 (1945).
13. ———, D. Friedland, and E. G. Scheibel, unpublished paper.
14. Perry, J. H., "Chemical Engineers' Handbook," 3 ed., McGraw-Hill Book Company, Inc., New York (1950).
15. Rao, M. N., private communication, Andhra University, Waltair, India.
16. Robinson, C. S., and E. R. Gilliland, "Elements of Fractional Distillation," 4 ed., McGraw-Hill Book Company, Inc., New York (1950).
17. Schwers, F., *J. chim. phys.*, **9**, 15 (1911).
18. Shilling, G. D., G. H. Beyer, and C. C. Watson, *Chem. Eng. Progr.*, **49**, 128 (1953).
19. Van Krevelen, D. W., and P. J. Hoftijzer, *Chem. Eng. Progr.*, **46**, 29 (1950).
20. White, R. R., *Petroleum Processing*, **1**, 147 (1946).
21. York, R., and R. C. Holmes, *Ind. Eng. Chem.*, **34**, 345 (1942).

Presented at A.I.Ch.E. Houston meeting